Electron Injection in Laser Plasma Accelerators by High-Order Field Ionization

M. Chen, E. Esarey, C. G. R. Geddes, C. B. Schroeder, and W. P. Leemans

Lawrence Berkeley National Laboratory, Berkeley, California 94720, USA

Abstract. Electron injection and trapping in a laser wakefield accelerator by high-order field ionization is studied theoretically and by particle-in-cell simulations. To obtain low energy spread beams we use a short region of gas mixture (H+N) near the start of the stage to trap electrons, while the remainder of the stage uses pure H and is injection-free. Effects of gas mix parameters, such as concentration and length, on the final electron injection number and beam quality are studied. Laser polarization and shape effects on injection number and final electron emittance are also shown.

Keywords: laser wakefield, injection, particle-in-cell simulation, ionization
PACS: 52.38.kd, 41.75.Jv, 52.65.Rr

INTRODUCTION

Laser-plasma accelerators (LPAs) [1] are of great interest because of their ability to sustain extremely large acceleration gradients, enabling compact accelerating structures. High-quality electron beams up to 1 GeV have been experimentally demonstrated in cm-scale plasma channels [2, 3]. In these channel-guided experiments the electron beam was created by trapping (self-injection) of background plasma electrons in the plasma wave. Both the quality and stability of the laser-plasma accelerated electron beams can be improved by using triggered injection methods to control the amount of trapped charge and the initial phase-space characteristics. Up to now, both laser-triggered methods [4, 5, 6] and plasma density tailoring [7, 8] have been proposed for controlled injection. Triggered injection into accelerating plasma waves via colliding laser pulses has been demonstrated experimentally [9]. Production of electron beams via plasma wave excitation on a negative density gradient has also been achieved [10].

In addition to the above injection methods, producing electrons at rest via ionization of the inner electrons of a high Z atom inside the wakefield can also be used to control injection. Chen *et al.* [11], discuss a scheme for ionization injection by use of two orthogonally directed laser pulses and a gaseous medium with a moderate or high atomic number (e.g., Neon). A pump laser pulse ionizes the medium to mid-charge states to form underdense plasma and excites a plasma wave to an amplitude below the self-trapping point. Another ultrashort laser pulse with higher intensity is then transversely injected, which further ionizes the medium to high-charge states producing unbound electrons. The newly ionized electrons can be trapped in the plasma wave and accelerated to high energies. Although the ionization injection was confirmed for this scheme by PIC simulations, electron acceleration in the transverse direction due to the transverse injection pulse is an issue [11]. Recently, two groups reported on the demonstration of ionization injection in laser wakefield acceleration [12, 13]. In these experiments, only one laser pulse was used both for wake excitation and ionization injection. Since a long mixed gas was used, final electron energy spread was quite large in these experiments. Furthermore, the ionization injection in these experiments depended critically on the self-focusing of the laser pulse, and the injection position, injection number, and beam quality were difficult to control.

In this paper we suggest using a two-stage gas jet to control ionization injection with a single laser pulse. The two-stage gas jet consists of an initially short section of high-Z gas (for injection into the plasma wave) followed by a long section of low-Z gas (for post-acceleration without additional trapping or dark current). We begin with a derivation of the trapping condition applied to ionization trapping, then present effects of the injection gas properties such as length and concentration, as well as effects of laser shape and polarization on the final beam quality.

TRAPPING CONDITION

From one dimensional wakefield theory, we know the Halmitonian of an electron $H = \gamma - \beta_p \gamma \beta_\parallel - \phi = const$, where β_p is the phase velocity of the wakefield, ϕ is its potential, γ is the relativistic factor of the electron and $\beta_\parallel$ is its

CP1299, *Advanced Accelerator Concepts: 14th Workshop*, edited by S. H. Gold and G. S. Nusinovich

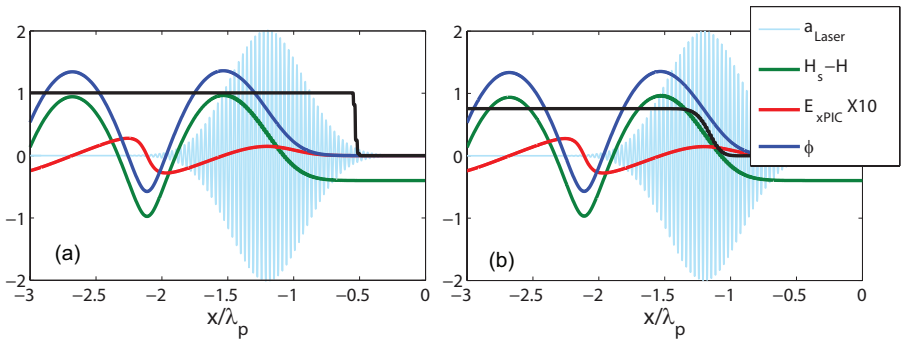

FIGURE 1. Vector potential of laser pulse (light blue line), wake potential (blue line), wake field (red line) and ionization rate (black line) along the longitudinal direction. The green line shows the trapping value $H_s - H$. (a) corresponds to the ionized electron of $N^{4+} \rightarrow N^{5+}$, and (b) corresponds to $N^{5+} \rightarrow N^{6+}$. Here $a = 2.0$, $L_{FWHM} = 14.89T_0$, and $n_e = 0.001 n_c$.

normalized longitudinal velocity. For an electron ionized at the position where the wake potential is $\phi(\xi_i)$, we have $H = H_0 = 1 - \phi(\xi_i)$. The injection condition is at the point where the wake potential is minimum (ϕ_{min}) such that the particle longitudinal velocity should satisfy $\beta_{\parallel} > \beta_p$. Therefore the trapping condition is $1 + \phi_{min} - \phi(\xi_i) \leq \sqrt{1 + p_{\perp}^2}/\gamma_p$. For a plane electromagnetic wave, the transverse canonical momentum is conserved $d_{\xi}(p_{\perp} - a_{\perp}) = 0$, with $\xi = z - \beta_p t$ and $a = eA/m_e c^2$ is the normalized vector potential. For an electron ionized at ξ_i, one has $p_{\perp}(\xi) = a_{\perp}(\xi) - a_{\perp}(\xi_i)$. If the electron is ionized at the position where the laser vector potential $a_{\perp}(\xi_i) \neq 0$, it will keep the initial perpendicular vector potential as the final transverse momentum [$p_{\perp} = a_{\perp}(\xi_i)$] after the laser pulse. So for the ionized electron to be trapped requires

$$H_i = 1 - \phi(\xi_i) \leq H_s = \gamma_{\perp}\gamma_p^{-1} - \phi_{\min} \tag{1}$$

where $\gamma_{\perp} = \sqrt{1 + p_{\perp}^2} = \sqrt{1 + a_{\perp}^2(\xi_i)}$. This trapping condition is the same as the condition given by Pak *et al.* [12], however, since we have assumed one dimensional geometry, the final transverse momentum here only comes from the ionization process. By considering the wake excitation by a resonant laser with a sine-profile with $a < 1$, the threshold of the laser pulse for trapping the electrons ionized at the peak is $0.64a^2 \geq 1 - \gamma_p^{-1}$, which indicates that the laser intensity must be relativistic for ionization-induced trapping [14].

The above analysis is based on the wake excitation and particle trapping. It shows that if the electron is born at a position (ξ_i) sufficiently behind the laser pulse front, the wake potential there $\phi(\xi_i)$ can be high enough to satisfy the trapping condition Eq.(1). These electrons will be decelerated less by the wakefield compared to an electron ionized at the head of the laser. The atomic potential keeps these electrons bound until the laser electric field is high enough to tunnel ionize. The atomic potential should be high enough to bind the electrons until an appropriate ξ_i, and it should not be too high, otherwise the ionization rate is too small. Nitrogen is an excellent source for injection, both for the theoretical and experimental considerations, when a 800nm laser pulse with normalized electric intensity of $a \sim 2$ is used. In Fig. 1(a) and (b) we show the injection possibility of the different valence electrons of Nitrogen. The light blue line shows the laser field, the blue line shows the wakefield potential and the red line shows the electric field of the wake, which are calculated by solving the 1D wakefield equations. Ionization degree is also shown by the black line. For each point, we calculate the $H_s - H$. As we see for the electrons ionized from $N^{4+} \rightarrow N^{5+}$, ionization mainly happens far in front of the laser peak and $H_s - H < 0$, hence no trapping happens. These electrons are ionized too earlier. For the inner electrons ($N^{5+} \rightarrow N^{6+}$), due to higher ionization potential, ionization has been moved to the peak of the laser pulse where $H_s - H > 0$ and electron trapping occurs.

EFFECTS OF GAS PROPERTIES ON FINAL BEAM QUALITY

To characterize beam quality available from ionization injection we performed particle-in-cell simulations with the explicit Particle-in-Cell code–VLPL [15], which includes ionization. In the simulations, the Ammosov-Delone-Krainov (ADK) ionization mechanism is applied in every simulation step to calculate the ionization of Nitrogen ions [16]. A short region of gas mixture (pre-ionized Hydrogen and neutral Nitrogen) near the start of the stage is used

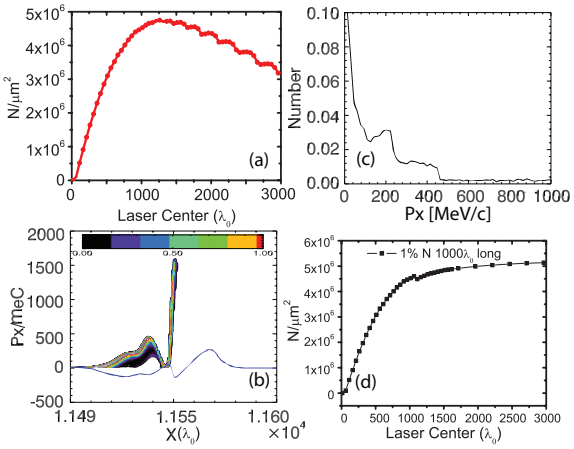

FIGURE 2. (a) Trapped electron number vs the length of the mixed gas traversed by laser pulse. (b) Distribution of electrons in the phase space (x-Px) and electric field of the wake. Many moderate energy electrons have slipped to the second bucket of the wake. (c) Electron energy spectrum at the dephasing length when a mixed gas with infinite length is used. (d) Trapped number evolution vs the laser propagation distance. Here the mixed gas length is fixed to be $1000\lambda_0$. Laser pulse: $a = 2.0$, $L_{FWHM} = 14.89T_0$, and the uniform plasma density $n_e = 0.001n_c$.

for electron injection, while the remainder of the stage uses pure (pre-ionized) Hydrogen gas that is injection-free due to the wake amplitudes selected. The electron density is set to be uniform in the pure Hydrogen region and the mixed gas region once all the outer 5 electrons of the nitrogen are ionized in the mixed gas region.

We first study the mixed gas length effect. To exclude effects due to different background electron density, in these simulations we fix the total ionized (until the 5th electron of Nitrogen) electron density to be $0.001n_c$, with $n_c = 1.7\times10^{21}cm^{-3}$ the critical density for a laser of $\lambda_0 = 800$nm wavelength, to see the injection number evolution. The normalized laser electric field is $a = 2.0$ and the FWHM of the pulse is $14.89T_0$ ($T_0 = \lambda_0/c = 2.67$fs), the same as the above theoretical calculations. The injected number is determined by counting the newly ionized electrons at each time step that satisfy the trapping condition $H < H_s$. Fig. 2(a) shows the relation between the injection number and the length of the mixed gas where the laser pulse has passed. When the gas length is small, the injection number linearly increases with the gas length. This saturates when the mixed gas is longer. It reaches a peak value (Q_s), then decreases. Hence, a too long mixed gas will not only prohibit further injection, but also make the initially injected electrons slip away from the wakefield and reduce the trapping number [see Fig. 2(b)]. Furthermore, too long a mixed gas region will result in a much wider final energy spectrum with low peak energy as shown in Fig. 2(c). When we increase the concentration of the Nitrogen to 2%, but fix other parameters (laser and ionized electron density), we find the maximum value of the trapped number is almost the same. It is only limited by the beam loading effect. In the simulations we see the higher the Nitrogen concentration the shorter the linear scaling region. The linear injection length (l_{linear}) depends on the Nitrogen concentration α_N and ionization degree [$\kappa(a_0)$]. They approximately satisfy the relation: $l_{linear} = Q_s/\kappa(a_0)\alpha_N$.

To avoid injection loss, one can adjust the length of the mixed gas. Fig. 2(d) shows the injection number vs the laser propagation distance. The mixed gas length here is $1000\lambda_0 = 800\mu m$. As expected, the cutoff of the mixed gas jet stops the further injection of newly ionized electrons from the front part of the wakefield. The slippage of the initially trapped electrons due to beam loading effect has also been stopped. Hence all the initially trapped electrons are kept in the wakefield.

To get a monoenergetic beam, simulations indicate that the mixed gas length should be even shorter than the cutoff length at which the maximum injection number is obtained. To clarify this, a scan of the mixed gas was conducted. Fig. 3(a) shows the final number (blue squares) and energy spread (black squares) of injected electrons when different mixture gas lengths are used. The laser intensity is $a = 2.0$ and the Nitrogen concentration is fixed at 1%. As we see, when the gas length is less than $1000\lambda_0$ long, the injected electron number is almost the same as the one we calculated from the potential method [see Fig. 2(a)]. However, the beam energy spread is almost 60% when the mixed gas length is $1000\lambda_0$ long. The energy spread has an approximately linear relationship with the mixed gas length. To get a high quality beam, one should reduce the gas length correspondingly.

We also fix the gas length to make a Nitrogen concentration scan. Fig. 3(b) shows the evolution of the injected

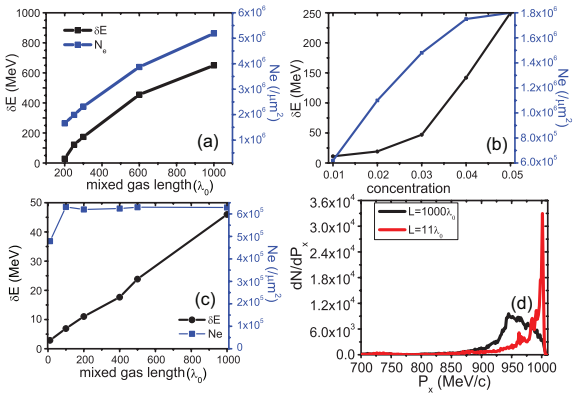

FIGURE 3. (a) Evolution of energy spread (black square point) and injected electron number (blue square point) along with the mixed gas length. Laser intensity: $a = 2.0$. (b) Dependence of energy spread and final electron injection number on the concentration of Nitrogen. Here the mixed gas length is $200\lambda_0$. Laser intensity: $a = 1.8$. (c) Dependence of energy spread and final electron injection number on the mixed gas length. Here the product of mixed gas length and concentration is fixed. Laser intensity: $a = 1.8$. (d) Final electron energy spectrum corresponding to the simulations of using different mixed gas length. Other parameters here are: $L_{FWHM} = 14.89T_0$, and the plasma density $n_e = 0.001n_c$.

electron number and beam energy spread when the gas length is $200\lambda_0$ long. When the concentration increases, both the injection number and energy spread increase. The injection number increases almost linearly, however, the energy spread increases dramatically after some point (3% here) due to beam loading effect. Comparing the length and concentration effects, we find that when the injection number is far away from the saturation value, the gas length effect is much more important than the concentration effect. Fig. 3(c) shows such kind of feature. In the simulations, we fix the product of concentration and mixed gas length. Since the injection number is in the linear regime, the final injection numbers are almost the same. The final energy spectrum width linearly increases with the gas length. Minimum energy spread can be obtained from the intercept of the curve, which is about 2.9MeV for a final beam energy of 1GeV. Two typical energy spectra are shown in Fig. 3(d) corresponding to the two points in Fig. 3(c). Again, we see the shorter the mixed gas the better the final beam energy spread.

EFFECTS OF LASER PROPERTIES ON FINAL BEAM QUALITY

To find the source of energy spread, we study the relationship of the electron final energy and the ionization phase (ξ_{ionize}) relative to the wakefield. Fig. 4(a) and (b) shows the distribution of the electron longitudinal momenta along their initial phase (ξ_{ionize}) at different times. As it shows, the final energy spectrum width comes from two contributions. One is the ionization distribution at different positions along the mixed gas. For the electrons that have the same value of ξ_{ionize}, the trajectory in the phase space is the same (assuming the beam loading effect is negligible.). Due to the different ionization time, they arrive at the peak energy at different times. This gives the slice energy spread shown in Fig. 4(a). The other energy spread source comes from the distribution at different ionization phases (ξ). Although some electrons have the same ionization position (x) in the lab frame, due to tunneling ionization mechanism, they have been ionized at different position related to the laser peak. This also means they have been injected at different phase (ξ) of the wake. They have different trajectories in the phase space. The maximum energies of these electrons are different. If we reduce the length of the mixed gas, the energy spread due to the first process can be reduced, however, the tunneling mechanism will determine the second energy spread. The minimum energy spread comes from this source, which can be seen in Fig. 4(b).

To minimize the energy spread, one can use different gas composition or tune the laser pulse to make the ionization near the flat-top of the wakefield. Here we show one example of a method to reduce the energy spread by use of a skewed laser pulse. Consider a laser pulse with the temporal profile $a(t) = a_0 \exp[-t^2/\tau^2(1+bt/\sqrt{t^2+\tau^2/4})]$. Here b is the skew parameter. When $b = 0$ it corresponds to a normal Gaussian pulse with $L_{FWHM} = \sqrt{2\ln 2}\tau$. In our simulations, we use $a_0 = 1.8$, $L_{FWHM} = 40$fs. Fig. 4(c) shows the laser profile and the electric field of the wakefield when a positive skew pulse is used. As comparison, we also use a negative skew pulse. In these simulations, we see that when a positive skewed laser pulse is used, the electrons are mainly ionized before the peak of the wakefield.

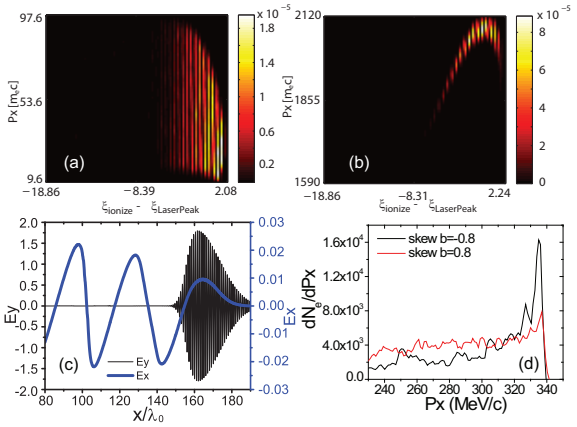

FIGURE 4. Electron energy distribution along their initial phase at time of $t = 800T_0$ (a) and $t = 1600T_0$ (b) for gaussian pulse. (c) Distribution of laser pulse (black thin line) and electric field of the wakefield (blue thick line) when a positive skewed laser pulse is used. (d) Electron energy spectrum in the cases of two different skewed pulses are used.

This results in a larger distribution of the electrons in the phase space of the wakefield. However, when a negative skewed pulse is used, ionization is tuned more deeply into the laser wakefield where the wake potential is much more flat. This reduces the volume of the electrons in the wake phase space. Since the different skewed pulses also excite different wakefields, comparison of the electron spectrum at the same acceleration length is difficult. Instead, we compare the spectrum at the same maximum electron energy and before the dephasing length to see the energy spread due to the ionization distribution. Fig. 4(d) shows the electron spectrum in these two different skew parameter cases. It shows, as predicted, that the positive skewed pulse gives a larger energy spread compared to the negative skewed pulse. To theoretically get an optimal laser pulse is quite difficult since both ionization and wake excitation should be considered. Here we only show in principle the possibility of reducing the energy spread by tuning the laser pulse. Note that the final energy spread at the dephasing length does not depend only on the ionization distribution, since wakefield evolution using different skew pulse is also different. For an injection electron source, pulse shaping is a useful method to get an initial high quality electron beam.

Transverse emittance is an important factor for a useful electron beam. In ionization injection, a source of transverse emittance is the residual transverse momentum from the ionization process [17]. Although from the ADK model, we see the electrons are mainly ionized at the peak of the electric field where the vector potential is zero, due to tunneling mechanism there are still some electrons ionized at a position of a non-zero vector potential. For a circularly polarized laser pulse, the laser vector potential is always nonzero at the ionization position. The vector potential at the ionization time will be reserved by the electrons and transformed to the final transverse momentum and increase the final beam transverse emittance. These phenomena have been demonstrated by our PIC simulations as shown in Fig. 5(a) and (b). To over come this in a single laser pulse case, one should make the ionization happen at the extreme point of the laser electric field. The simplest way of doing this is tuning of the laser intensity. Fig. 5(c) and (d) show the final injection number and average transverse momentum of the electrons at different laser intensities, respectively. Lower laser intensity gives smaller transverse emittance, however, it also gives smaller injection number. As a compensation, one can increase the gas concentration to get the same injection number.

SUMMARY

By using ionization included PIC simulations, we studied electron injection due to ionization from high Z atoms in laser wakefield acceleration. A two-stage injection-acceleration structure is used to get high quality electron beams. Both gas and laser effects on the final beam quality such as beam charge, energy spread, and emittance were investigated. We have also conducted multi-dimensional simulations to characterize the injection process. In the multi-dimensional case, simulations show ionization injection is still possible and the fundamental findings of current work are still meaningful. Other effects such as the injection trajectory and source of final transverse emittance require consideration of multi-dimensional effects. These will appear in a future publication [14].

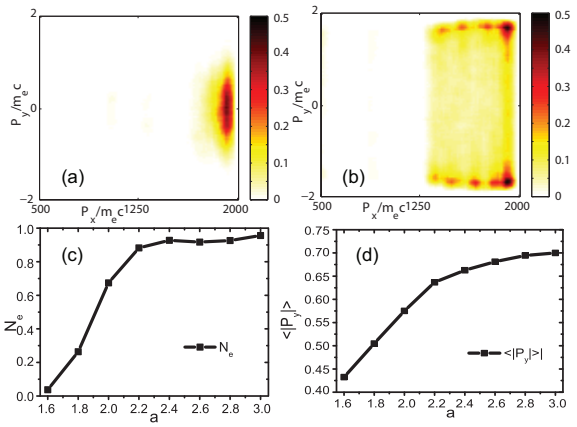

FIGURE 5. Electron transverse momenta distribution when a linearly polarized laser pulse (a) or a circularly polarized pulse (b) is used. Here laser pulse: $a = 1.8$, $L_{FWHM} = 14.89T_0$, and the uniform plasma density $n_e = 0.001n_c$. (c) Injection number and (d) average normalized transverse momenta dependence on laser intensity for a linearly polarized laser pulse.

ACKNOWLEDGMENTS

This work was supported by the Director, Office of Science, Office of High Energy Physics, of the U.S. Department of Energy under Contract No. DE-AC02-05CH11231 and by the National Science Foundation. Resources of the National Energy Research Scientific Computing Center are used to carry out the simulations.

REFERENCES

1. E. Esarey, C. B. Schroeder, and W. P. Leemans, *Rev. Mod. Phys*. **81**, 1229 (2009).
2. W. P. Leemans, B. Nagler, A. J. Gonsalves, C. Tóth, K. Nakamura, C. G. R. Geddes, E. Esarey, C. B. Schroeder, and S. M. Hooker, *Nature Phys.* **2**, 696 (2006).
3. K. Nakamura, B. Nagler, C. Tóth, C. G. R. Geddes, C. B. Schroeder, E. Esarey, W. P. Leemans, A. J. Gonsalves, and S. M. Hooker, *Phys. Plasmas* **14**, 056708 (2007).
4. E. Esarey, R. F. Hubbard, W. P. Leemans, A. Ting, and P. Sprangle, *Phys. Rev. Lett.* **79**, 2682 (1997).
5. C. B. Schroeder, P. B. Lee, J. S. Wurtele, E. Esarey, and W. P. Leemans, *Phys. Rev. E* **59**, 6037 (1999).
6. G. Fubiani, E. Esarey, C. B. Schroeder, and W. P. Leemans, *Phys. Rev. E* **70**, 016402 (2004).
7. S. Bulanov, N. Naumova, F. Pegoraro, and J. Sakai, *Phys. Rev. E* **58**, R5257 (1998).
8. P. Tomassini, M. Galimberti, A. Giulietti, D. Giulietti, L. A. Gizzi, L. Labate, and F. Pegoraro, *Phys. Rev. ST Accel. Beams* **6**, 121301 (2003).
9. J. Faure, C. Rechatin, A. Norlin, A. Lifschitz, Y. Glinec, and V. Malka, *Nature* **444**, 737 (2006); C. Tóth, E. Esarey, C.G.R. Geddes, W.P. Leemans, K. Nakamura, D. Panasenko, C.B. Schroeder, *Proc. Particle Accel Conference*, Albuquerque NM, pp. 2975-77 (2007); G. Plateau, *et al.*, in these proceedings.
10. C. G. R. Geddes, K. Nakamura, G. R. Plateau, Cs. Tóth, E. Cormier-Michel, E. Esarey, C. B. Schroeder, J. R. Cary, and W. P. Leemans, *Phys. Rev. Lett.* **100**, 215004 (2008).
11. M. Chen, Z.-M. Sheng, Y.-Y. Ma, and J. Zhang, *J. Appl. Phys.* **99**, 056109 (2006).
12. A. Pak, K.A. Marsh, S.F. Martins, W. Lu, W.B. Mori, and C. Joshi, *Phys. Rev. Lett.* **104**, 025003 (2010).
13. C. McGuffey, A.G.R. Thomas, W. Schumaker, *et al.*, *Phys. Rev. Lett.* **104**, 025004 (2010).
14. M. Chen, E. Esarey, C.G.R. Geddes, C.B. Schroeder, and W.P. Leemans, to be submitted (2010).
15. A. Pukhov, *J. Plasma Phys.* **61**, 425 (1999).
16. N. B. Delone and V. P. Krainov, *J. Opt. Soc. Am. B* **8**, 1207 (1991).
17. W.P. Leemans *et al.*, *Phys. Rev. Lett.* **68**, 321 (1992); W.P. Leemans *et al.*, *Phys. Rev. A* **46**, 1091 (1992).